Crystal-size distributions and possible biogenic origin of Fe sulfides

MIHÁLY PÓSFAI[1], KRISZTINA CZINER[1], EMÖ MÁRTON[2], PÉTER MÁRTON[3], PETER R. BUSECK[4], RICHARD B. FRANKEL[5] and DENNIS A. BAZYLINSKI[6]

[1]Department of Earth and Environmental Sciences, University of Veszprém, Veszprém, POB 158, H-8200 Hungary
[2]Paleomagnetic Laboratory of the Eötvös Loránd Geophysical Institute, Budapest, Homonna u. 1., H-1118 Hungary
[3]Department of Geophysics, Eötvös Loránd University, Budapest, Ludovika tér 1., H-1088 Hungary
[4]Departments of Geological Sciences and Chemistry/Biochemistry, Arizona State University, Tempe, Arizona 85287-1404, USA
[5]Department of Physics, California Polytechnic State University, San Luis Obispo, California 93407, USA
[6]Department of Microbiology, Iowa State University, Ames, Iowa 50011, USA

Abstract: Sedimentary greigite (Fe_3S_4) can form either by "biologically controlled" or by "biologically induced mineralization" (BCM and BIM, respectively). In order to identify the origin of magnetic Fe sulfides, we studied and compared the sizes and morphologies of greigite crystals produced by a magnetotactic microorganism (previously described and referred to as the "many-celled magnetotactic prokaryote", MMP) and Fe sulfides from two specimens of Miocene sedimentary rocks (from Łąka, in the foredeep of the Western Carpathians and from Michalovce, in the Transcarpathian Depression). Greigite grains from the MMP and the Łąka rock show nearly Gaussian crystal-size distributions (CSDs), whereas the CSD is lognormal for Fe sulfides from the Michalovce rock. We simulated various crystal-growth mechanisms and matched the calculated and observed CSDs; crystals from the MMP and the Łąka rock have CSDs that are consistent with random growth of crystal nuclei in an open system, whereas the CSD of the Michalovce Fe sulfides is consistent with surface-controlled growth followed by supply-controlled growth in an open system. On the basis of CSDs and characteristic contrast features in the transmission electron microscope, greigite in the Łąka rock is likely of BCM origin, whereas the Fe sulfide crystals in the other rock sample were produced by BIM processes. Our results indicate that the methods we applied in this study may contribute to the identification of the origin of magnetic Fe sulfide minerals in sedimentary rocks.

Key-words: greigite, magnetotactic bacteria, biologically controlled mineralization, biologically induced mineralization, crystal size distribution.

Introduction

Fine-grained magnetic minerals in sediments and sedimentary rocks include Fe oxides and sulfides such as magnetite (Fe_3O_4) and greigite (Fe_3S_4). The origin of these minerals is unkown in many cases; magnetite can be produced by both biogenic and inorganic processes, whereas sedimentary greigite likely forms as a result of biogenic processes. Microorganisms mediate the formation of minerals in two different ways: in "biologically controlled mineralization" (BCM)

the crystals form inside the living cell, whereas in "biologically induced mineralization" (BIM) they form outside or on the cell as a result of the indirect effect of the microorganism's metabolism (Lowenstam & Weiner, 1989). Apart from a study that showed the presence of presumably BCM greigite in soil (Stanjek *et al.*, 1994), we do not have direct evidence that greigite of BCM origin influences the magnetic properties of sediments and rocks. The goal of this study is to establish criteria that could be used for identifying BCM greigite in geological specimens.

BCM greigite is known to be produced by magnetotactic bacteria (Mann *et al.*, 1990; Farina *et al.*, 1990; Heywood *et al.*, 1990). Such microorganisms obtain an evolutionary advantage by forming intracellular, single-domain magnetic crystals that cause the bacteria to be oriented in the Earth's magnetic field (Frankel *et al.*, 1997). Magnetotactic bacteria generally produce either magnetite or greigite with only one morphological type described to date that produces both (Bazylinski, 1999). Although most studies on magnetotactic bacteria were performed on magnetite-producing species, several studies addressed the physical and chemical properties and formation mechanisms of greigite magnetosomes (Heywood *et al.*, 1991; Pósfai *et al.*, 1998a and b; Lins *et al.*, 2000); from these we know that BCM greigite crystals are characterized by a size range from about 30 to 150 nm, an abundance of defects, and a typical spotty contrast in transmission electron microscope (TEM) images.

Greigite can also form in sediments as a result of BIM processes. Owing to the metabolism of sulfate-reducing bacteria, H_2S is present at the level of the OATZ (Oxic-Anoxic Transition Zone) and below. By the reaction of H_2S and HS^- with dissolved Fe, amorphous FeS precipitates. Through a series of solid-state transformations, the amorphous precipitate converts to mackinawite (tetragonal FeS) and then either to greigite or pyrite (Morse *et al.*, 1987; Schoonen & Barnes, 1991; Rickard, 1997). Organisms play a role in creating the chemical environment that is necessary for Fe sulfide formation during this process, but they do not control the growth of greigite particles. As a consequence, such particles likely have a broad size distribution, and their spatial arrangement is non-specific (Bazylinski & Moskowitz, 1997). Although much research has been done to describe the conditions and kinetics of the formation of BIM Fe sulfides (Rickard, 1995, 1997; Rickard & Luther, 1997), physical properties such as crystal-size distributions and microstructural features of sedimentary BIM greigite remain unknown.

Greigite has been increasingly reported as the main carrier of magnetic remanence in sedimentary rocks (Krs *et al.*, 1992; Roberts, 1995; Jelinovska *et al.*, 1998). For the paleomagnetic interpretation of rock magnetism it is of importance whether the greigite formed by BIM processes or was deposited within magnetotactic bacteria. When these bacteria die, they eventually lyse and their magnetosomes become dispersed and are deposited either in random orientations or oriented by the Earth's magnetic field. On the other hand, BIM greigite is produced at the sediment surface or at a moderate burial depth, and the question is when these crystals acquired their chemical remanence. In either case, it is not straightforward to determine whether the primary magnetic-field direction is preserved in the greigite crystals.

Bulk magnetic methods are useful for identifying ferrimagnetic Fe sulfides, particularly greigite (the most recent compilation was published by Sagnotti & Winkler, 1999); however, these studies do not provide information regarding the origin of greigite. Bulk magnetic methods can be used to detect the presence of single-domain crystals. In the case of sedimentary magnetite, single-domain grains are usually interpreted as formed by BCM processes. Since the single-domain size range extends to quite large sizes in greigite (up to about 0.8 μm, Hoffmann, 1992), and both BIM and BCM processes produce greigite that is primarily single-domain, bulk magnetic methods do not seem to be very useful for distinguishing BCM from BIM greigite.

Since the finding of nanoscale magnetite crystals that were interpreted as possible traces of fossil life in a Martian meteorite (McKay *et al.*, 1996), there is strong interest in defining criteria that can be used for identifying biogenic minerals in rocks. Several characteristics of BCM magnetite were recently listed by Thomas-Keprta *et al.* (2000). These include (1) constrained size (single-domain) and aspect ratios, (2) chemical purity, (3) defect-free structure, (4) occurrence of crystals in chains, (5) unusual crystal morphology, and (6) crystal elongation along specific crystallographic directions. Thomas-Keprta *et al.* (2000) described a crystal population in the meteorite ALH84001 that is similar to magnetite produced by the magnetotactic bacterium strain MV-1 with respect to five of the above six criteria. In our view, criterion (3) may not be useful for identifying BCM magnetite, since several magnetotactic strains are

known to produce twinned crystals (Devouard *et al.*, 1998). Also, as Thomas-Keprta *et al.* (2000) noted, even bacterial crystals are not expected to occur in chains once they had been deposited in the sediment after the host bacterium died. Criteria (1), (2), (5), and (6) may be the most useful for distinguishing BCM magnetite.

In addition to the above criteria, the shape of the crystal-size distribution (CSD) can be used for identifying BCM minerals. Certain crystal nucleation and growth processes are known to produce distinct CSDs (Eberl *et al.*, 1998). For example, in an open system surface-controlled growth yields lognormal distributions, whereas in a closed system supply-controlled ripening processes produce more symmetric or even negatively-skewed CSDs (Eberl *et al.*, 1998). Previous studies of BCM magnetite showed that the CSDs are typically negatively skewed, with sharp cutoffs towards larger sizes (Devouard *et al.*, 1998), and could be best simulated as if the crystals grew by Ostwald ripening (Eberl & Frankel, 1999). CSDs of magnetite from some magnetotactic bacteria display two maxima, indicating the role of agglomeration during crystal growth; this process may be responsible for the occurrence of twinned crystals (Arató *et al.*, 2000).

Similar information on the CSDs of Fe sulfides from magnetotactic bacteria is completely lacking. Therefore, the main goals of the present paper are to characterize the sizes and morphologies of Fe sulfide crystals from a magnetotactic organism, the MMP, and to compare the results with CSDs obtained from Fe sulfides that occur in sedimentary rocks**.** The analysis of CSDs provides information regarding the formation mechanism of Fe sulfides in magnetotactic bacteria and can be helpful for identifying BCM greigite in sedimentary rocks.

Experimental

Cells of the MMP were collected at Parker River Wildlife Refuge, Rowley, MA, and Sweet Springs Nature Preserve, Morro Bay, CA (Pósfai *et al.*, 1998b). In the present study we analyzed the morphologies of the Fe sulfide magnetosomes in the cells of the MMP. The phase transformations, microstructural features, and compositions of the Fe sulfide crystals were described in detail in previous studies (Pósfai *et al.*, 1998a and b).

Two rock samples were used for this study; these specimens were selected from half a dozen sedimentary rock samples that were expected to contain greigite on the basis of bulk magnetic measurements. Both specimens are Miocene marls, one from Łąka (Poland) in the foredeep of the Western Carpathians, and the other from Michalovce (Slovakia) in the Transcarpathian Depression. The Łąka marl deposited in a brackish environment, whereas the Michalovce rock formed in a hypersaline basin.

Bulk magnetic experiments included the measurement of the natural remanent magnetization (NRM) and the susceptibility in the natural state, and the stepwise thermal demagnetization of the NRM followed by the remeasurement of both the NRM and the susceptibility after each heating step. We also measured the magnetization of specimens in an increasing steady magnetic field (up to 1.0 T) at room temperature (IRM acquisition), and the magnetization of the same specimens along three mutually perpendicular axes in fields of 1.0, 0.36 and 0.2 T, respectively (3-component IRM). Finally, we performed a stepwise thermal demagnetization of the 3-component IRM, followed by the remeasurement of the IRM and the susceptibility after each heating step.

For TEM studies, fragments of the rocks were crushed under ethanol, and magnetic mineral grains were collected on holey-carbon-covered TEM grids using a bar magnet to attract magnetic particles from the suspension onto the grid. We used a Philips CM20 TEM operated at 200 kV accelerating voltage for obtaining TEM micrographs and selected-area electron-diffraction (SAED) patterns from the Fe sulfide grains in the two rock samples. Chemical analysis using energy-dispersive X-ray spectrometry (EDS) was performed using a Noran Voyager spectrometer attached to the TEM; we used the EDS spectra for a qualitative identification of the Fe sulfides.

The dimensions of the Fe sulfide crystals were measured on digitized electron micrographs using Digital Micrograph 3.0 (Gatan, Inc.) software. We matched the observed CSDs with simulated curves that were calculated for distinct crystal nucleation and growth mechanisms using the GALOPER (Growth According to the Law of Proportionate Effect) computer program of Eberl *et al.* (1998, 2000).

Results

Magnetic measurements

The isothermal remanent magnetization (IRM) acquisition curves for the two rock samples are

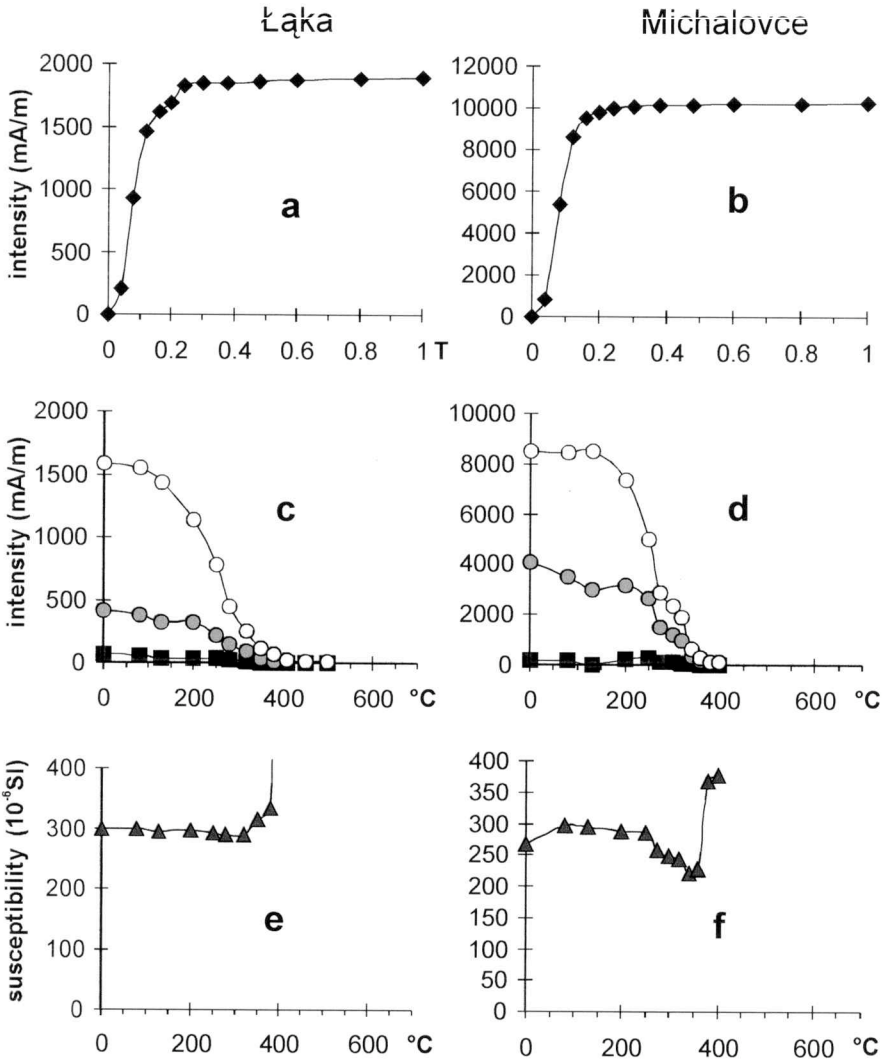

Fig. 1. Results of bulk magnetic experiments on rock samples from Łąka (a, c, e) and Michalovce (b, d, f). (a) and (b) Magnetization in a field increasing up to 1.0 T at room temperature (IRM acquisition); (c) and (d) stepwise thermal demagnetization of the 3-component IRM; (e) and (f) changes in susceptibility upon heating. (The symbols on the curves mark individual measurements.)

typical of greigite, since the increase is at first slow, and saturation is reached in a relatively low field (Fig. 1a and b). The intensities of both the NRM and the IRM are high relative to the respective susceptibilities (e and f), again typical for magnetic Fe sulfides. The thermal demagnetization curves of both the NRM (not shown) and the 3-component IRM (c and d) show a decrease in intensity from 200°C on, and an important unblocking at 360°C. These values are typical of greigite (Sagnotti & Winkler, 1999); the gradual decay of magnetization above 200°C is attributable to the onset of thermal decomposition of greigite. The presence of minor amounts of other ferrimagnetic Fe sulfides cannot be entirely excluded: the low and intermediate coercivity components of the composite IRM show a step-like decrease in the Michalovce sample (d) that

may result from the alteration of a ferrimagnetic phase other than greigite. The same IRM components indicate a sluggish decomposition in the Łąka sample (c). Because the heating experiments were performed in air, the susceptibility curves for both samples (e and f) show a sudden increase above 380°C, indicating the oxidation of the Fe sulfides and the formation of a new magnetic phase, probably magnetite. Prior to the increase, a significant decrease in susceptibility is observed for the Michalovce rock (typical of greigite), whereas a similar decrease is inconspicuous for the Łąka rock (e), *i.e.*, the latter deviates considerably in this respect from the expected pattern. The NRM versus temperature curves (not shown in the figure) are similar to the decay curves of the soft and medium-hard components of the IRM of the respective samples, indicating that the iron sulfides carry ancient magnetic signals at both Łąka and Michalovce.

TEM studies

Bacterial sulfides from the MMP

The results of TEM observations of Fe sulfides from the MMP were presented in detail earlier (Pósfai *et al.*, 1998a and b). According to these studies, magnetotactic bacteria produce another Fe sulfide mineral, mackinawite (FeS), in addition to greigite. Non-magnetic mackinawite forms first and then converts to ferrimagnetic greigite. As a result of this solid-state transformation, greigite crystals typically contain numerous defects, giving rise to spotty (strain) contrast in the TEM (Fig. 2). The speed of the conversion is unknown, but it must be rapid in the natural environment because most crystals are greigite; only very few of them are mackinawite. The morphologies of the Fe sulfides are quite variable, even within the same cell (Fig. 2). These results were based on observations of several types of magnetotactic bacteria. However, in the present study we used the electron micrographs that were obtained from the MMP only, in order to have morphological data on magnetosomes from cells that belong to the same type of microorganism (DeLong *et al.*, 1993).

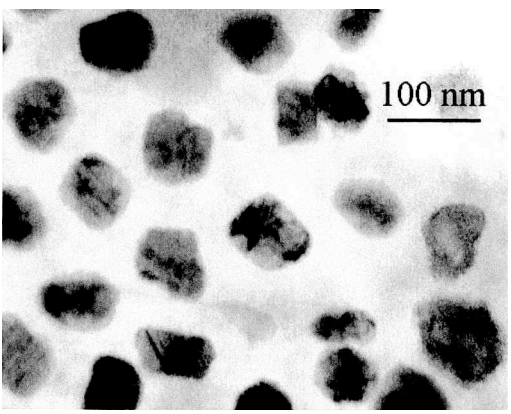

Fig. 2. Typical BCM greigite crystals from the multicellular magnetotactic prokaryote (MMP), showing irregular shapes and spotty contrast.

The sizes and shapes of the magnetosome crystals were measured on digitized TEM micrographs by fitting ellipses to the two-dimensional TEM projections of the Fe sulfide crystals. The long and short axes of the best-fitting ellipse were taken as the length and width of the crystals, respectively. Errors arise from the uncertainty of using two-dimensional data from unknown orientations of three-dimensional crystals (Devouard *et al.*, 2000) and from the approximation of irregular crystal outlines by ellipses. However, these errors were found to be small (Devouard *et al.*, 1998), and the data allow us to make a consistent statistical evaluation of crystal dimensions in distinct samples. Since we used the same method as Devouard *et al.* (1998) for measuring magnetite magnetosomes, our results are directly comparable with data on bacterial magnetite.

We measured the dimensions of 411 crystals and plotted their frequencies as a function of length, width, average diameter ((length +width)/2), and shape factor (width/length) (Fig. 3). The shape-factor diagram provides information on the degree of elongation, whereas the three size-distribution histograms can be used for making comparisons among crystal populations from different samples and for deciphering possible crystal-growth processes.

The size-distribution diagrams (Fig. 3a, b, and c) all show almost perfectly bell-shaped, Gaussian CSDs. The crystal-width distribution (b) is narrower than the length distribution (a) and appears to have two maxima. The average sizes of the crystals (c) vary from 25 to 100 nm, with the maximum of the size distribution at 60 to 65 nm. The shape-factor diagram (d) indicates that the morphologies of the crystals are not as constrained as in magnetite-producing bacteria: both highly elongated (shape factor 0.3) and almost spherical (shape factor > 0.95) crystals occur, and the frequency of crystal shapes is roughly the same from 0.6 to 0.9.

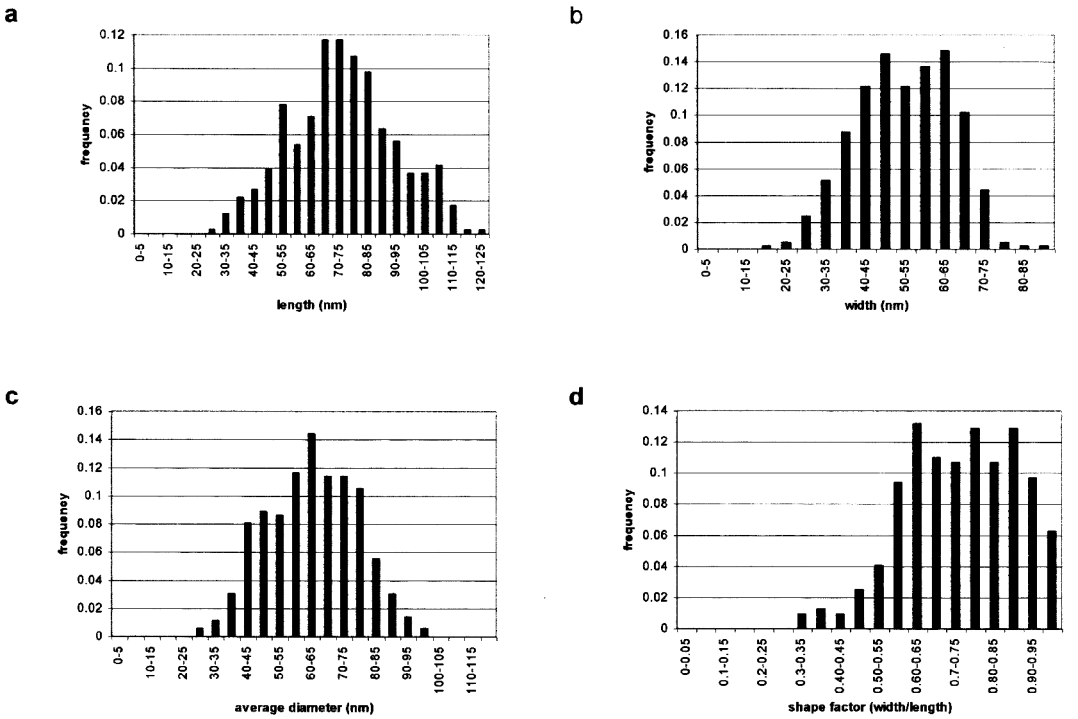

Fig. 3. Size (a, b, c) and shape (d) distributions of greigite crystals from cells of the multicellular magnetotactic prokaryote (MMP).

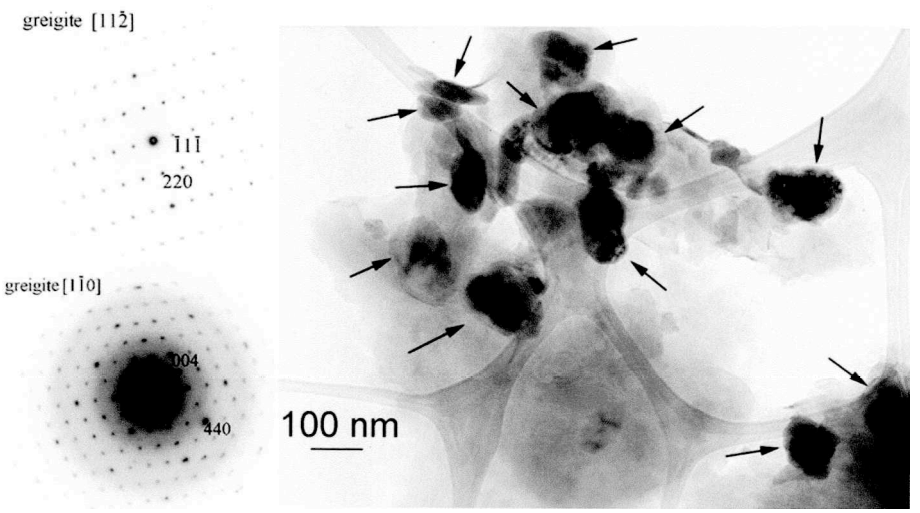

Fig. 4. Greigite crystals (arrowed) from the Łąka specimen, lying on the surface of a clay mineral (light grey sheet). The lacey film in the background is the holey-carbon supporting substrate. The selected-area electron diffraction patterns were obtained from two different greigite crystals in the image.

Greigite from the Łąka marl

In the Łąka specimen Fe sulfide crystals occur in clusters attached to the surfaces of clay minerals. In bright-field, amplitude-contrast TEM images the Fe sulfides appear as dark grains on a background of lighter sheets of clay minerals (Fig. 4). SAED patterns were obtained from several crystals and all are consistent with greigite (Fig. 4). They typically show uneven, spotty contrast in the bright-field images, resembling the bacterial Fe sulfides from the MMP.

The statistical analysis of crystal dimensions reveals that the crystals are about twice as large as in the MMP (Fig. 5). The length (a) and average size distributions (c) show slightly positively skewed distributions. The shape-factor diagram indicates that greigite crystals lack a specific morphology in this sample, just as in the case of the MMP greigite; nevertheless, there is a more distinct maximum in this curve (d) than in the shape distribution of the bacterial greigite (Fig. 3d). The irregular shapes of the crystals are also apparent in the TEM images (Fig. 4).

Fe sulfides from the Michalovce marl

Fe sulfide crystals from this specimen are clustered in large groups (Fig. 6). The appearance of the grains is quite different from that in the MMP or in the Łąka specimen: the crystals are mostly euhedral and show uniform contrast in the TEM. In addition, pyrite as well as greigite occurs. The sample preparation method did not permit the observation of their relative spatial distribution.

Statistical analysis of crystal sizes is difficult because of the aggregation of Fe sulfides into large groups. Crystals that are larger than indicated in Fig. 7 also occur, but we did not measure them because it was not certain whether they are single crystals or large aggregates of smaller ones. All three size distributions (length, width and average, (a), (b) and (c), respectively) show positively skewed, lognormal distributions. The maximum of

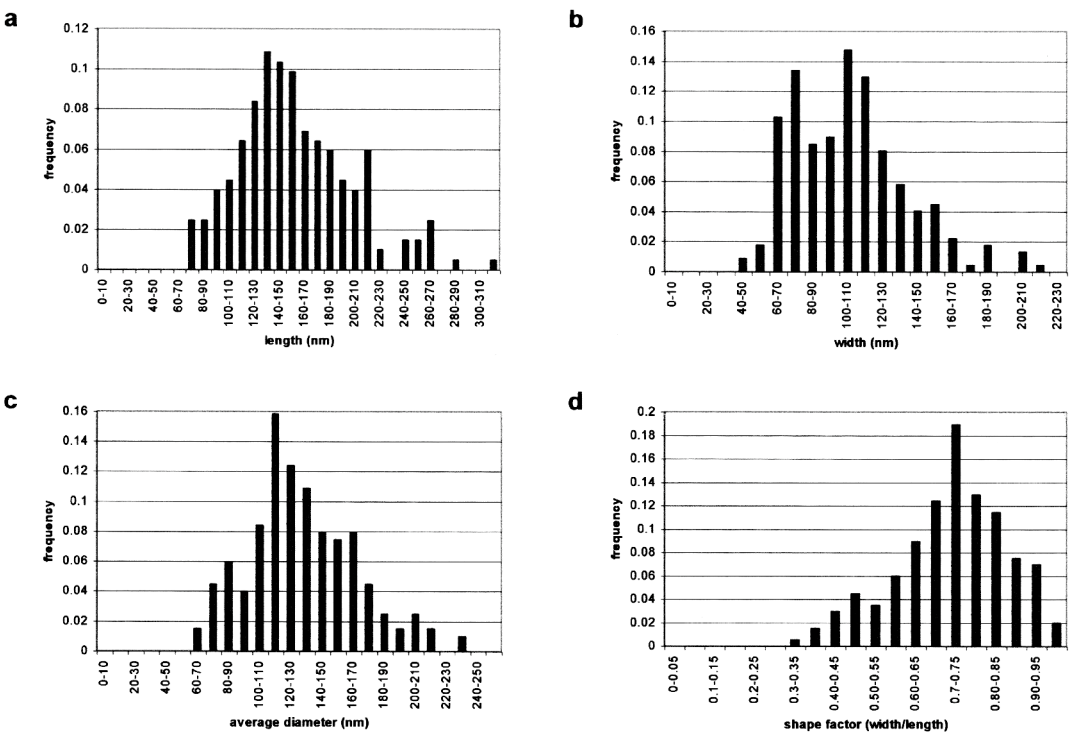

Fig. 5. Size (a, b, c) and shape (d) distributions of greigite crystals from the Łąka specimen.

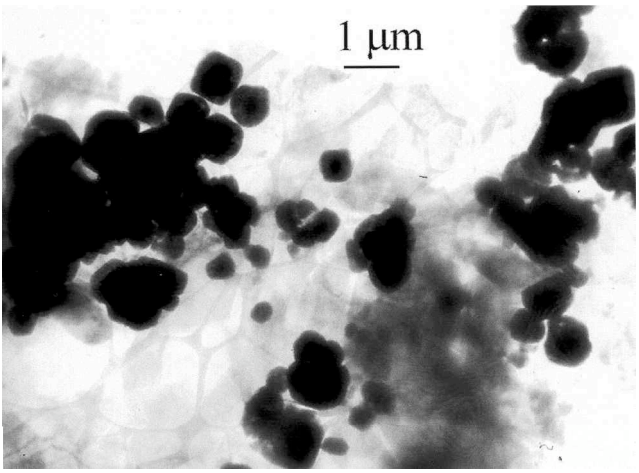

Fig. 6. Greigite and pyrite crystals (dark grains) from the Michalovce specimen, showing euhedral morphology and uniform black contrast.

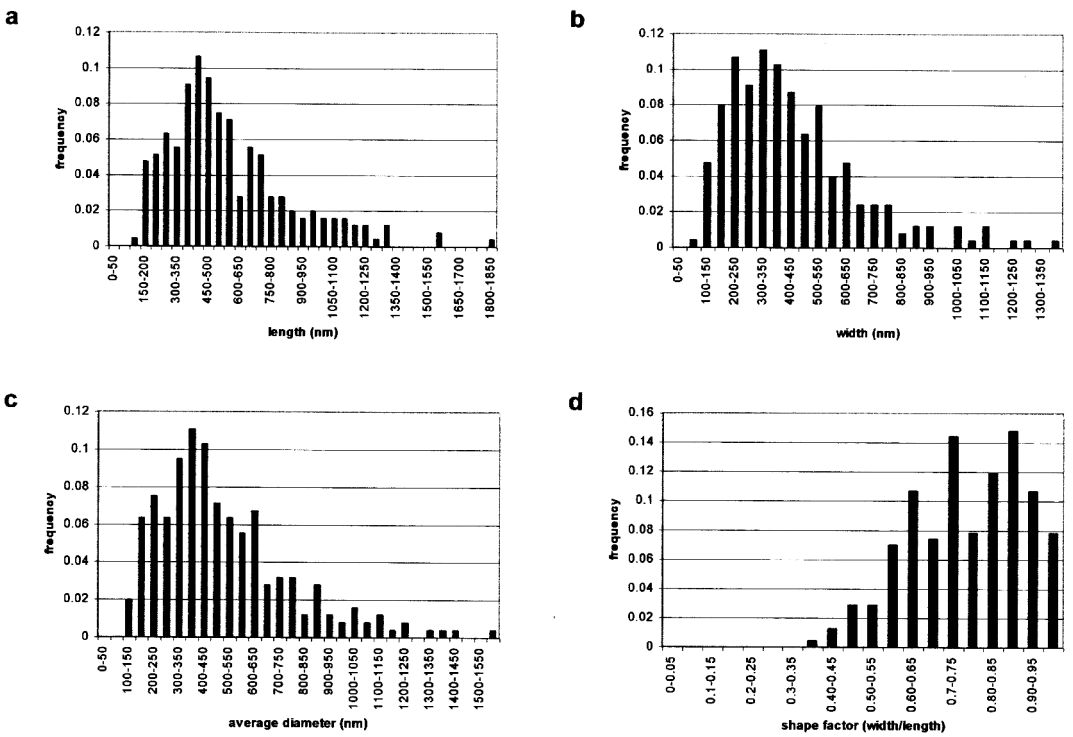

Fig. 7. Size (a, b, c) and shape (d) distributions of Fe sulfide crystals from the Michalovce specimen.

the average CSD curve is between 400 and 450 nm; thus, the Fe sulfide crystals are significantly larger in this specimen than in the MMP or in the Łąka rock. The broad shape distribution (d) indicates irregular crystal morphologies, similar to the other two specimens.

Discussion and conclusions

Crystal-growth simulations

Different crystal nucleation and growth processes produce CSDs that have distinctive shapes (Eberl *et al.*, 1998; Kile & Eberl, 1999); thus, observed CSDs convey information about the growth history of natural crystal populations. In a model that was developed by Eberl *et al.* (1998, 2000) and incorporated in the computer program GALOPER, the growth of linear crystal dimensions is simulated for a variety of mechanisms, including surface-controlled, supply-controlled, and random growth in an open system, and Ostwald and kinetic ripening in a closed system. GALOPER has been used to deduce the growth histories of a variety of minerals from many types of geological settings (Eberl *et al.*, 1998; Kile & Eberl, 1999; Eberl & Frankel, 1999; Srodon *et al.*, 2000) and is used in this study to simulate growth mechanisms for the three studied Fe sulfide samples.

If there is an unlimited supply of nutrients and the rate of growth depends on the previous size of the crystal, the growth mechanism is termed "surface-controlled" and can be simulated in GALOPER according to the Law of Proportionate Effect (LPE):

$$X_{J+1} = X_J + \varepsilon_J X_J,$$

where X_J is the linear crystal dimension after J calculation cycles. The many factors that govern the variability of the system are condensed into ε_J, a random number that is allowed to vary between 0 and 1 (Eberl *et al.*, 1998). If the volume of reactants in an open system is limited, the growth mechanism is termed "supply-controlled" and is simulated using a modified form of the LPE equation:

$$X_{J+1} = X_J + v_J \varepsilon_J X_J,$$

where v_J is a fraction that is a function of the volume available during each growth cycle for each crystal (Eberl *et al.*, 2000). "Random growth" occurs when the amount of material added to the crystal in each cycle is independent of the crystal's previous size and is not limited by the availability of nutrients (Eberl *et al.*, 2000):

$$X_{J+1} = X_J + \varepsilon_J.$$

GALOPER simulations of crystal growth mechanisms in a closed system include "Ostwald ripening" (when crystals having sizes smaller than a critical diameter dissolve and larger crystals grow), "random ripening" (when crystals dissolve randomly with respect to size), and crystal coalescence. During the ripening processes the dissolved crystals supply material for the growth of the remaining crystals.

Changes in the CSD can be characterized by the evolution of the parameters α and β^2, where α is the mean of the natural logarithms of the sizes and β^2 is the variance of the natural logarithms of the sizes. If f(X) is the frequency of group size X, then:

$$\alpha = \sum \ln(X) f(X);$$
$$\beta^2 = \sum (\ln X - \alpha)^2 f(X).$$

Thus, α is a function of the mean size, and β^2 is a function of the shape of the CSD (Eberl *et al.*, 1998). During surface-controlled growth in an open system β^2 increases, producing a positively skewed, lognormal CSD. Supply-controlled and random growth processes in an open system tend to preserve the β^2 value of the original CSD that formed on nucleation, whereas Ostwald ripening in a closed system decreases β^2 and can produce negatively skewed CSDs (Eberl *et al.*, 1998).

The statistical details of the Fe sulfide CSDs from the three samples show some characteristic differences (Table 1). Because of the irregular shapes of the crystals we chose the average CSDs for a detailed analysis (the row set in boldface in

Table 1. Statistical data for the size distributions of Fe sulfide crystals.

Sample	Distribution	Mean (nm)	Standard deviation	Skewness	α	β^2	Simulated growth mechanism
MMP (bacterial greigite; 411 crystals)	length	74	18	0.1			random growth in an open system
	width	52	12	-0.1			
	average	**63**	**14**	**0.0**	**4.115**	**0.055**	
Łaka (greigite; 216 crystals)	length	153	51	1.1			random growth in an open system
	width	108	36	1.1			
	average	**129**	**35**	**0.5**	**4.857**	**0.070**	
Michalovce (greigite and pyrite; 253 crystals)	length	490	300	1.3			surface- then supply-controlled growth in an open system
	width	376	234	1.3			
	average	**433**	**266**	**1.3**	**6.077**	**0.273**	

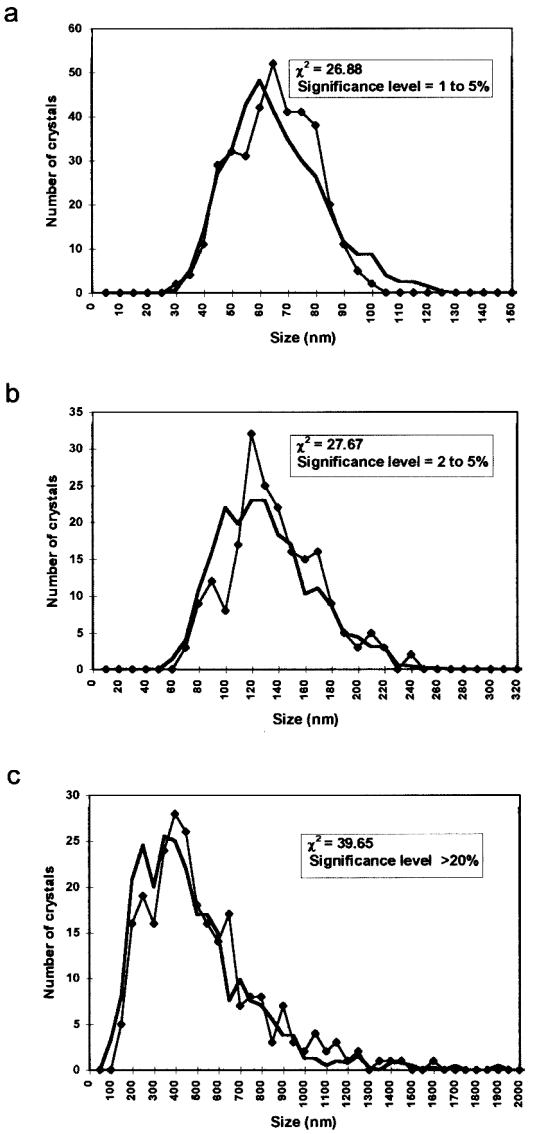

Fig. 8. A comparison of observed and calculated CSD curves. The observed distributions are marked by small squares (see text). (a) Greigite from the MMP; (b) greigite from the Łąka specimen; (c) Fe sulfides from the Michalovce specimen.

Table 1). In the GALOPER simulations our goal was to match the observed and calculated values of α and β^2. The simulated and observed distributions were compared using the χ^2-test; we obtained a significance level > 1 % for all three specimens, indicating that the calculated and observed distributions may differ only by statistical fluctuations (Fig. 8).

For the MMP greigite the best match between calculated and observed CSDs (Fig. 8a) could be obtained using GALOPER's "random growth in the open system" option, which simulates crystal growth by the addition of random amounts of material to the crystal surfaces. We chose a critical nucleus diameter of 3 nm, and simulated one cycle of "nucleation and surface-controlled growth," which resulted in an initial crystal population having a lognormal CSD and a mean size of about 9 nm. These crystals were then grown using the random-growth simulation, as long as the CSD reached α and β^2 values that closely matched the observed ones. During random growth β^2 decreased, resulting in a nearly Gaussian distribution. We certainly cannot exclude the possibility that other growth mechanisms can produce the same CSD. However, we simulated many other processes and pathways of crystal growth (both in open and closed systems), and all failed to produce a match between observed and calculated CSDs at a level of significance better than 1 % in the χ^2-test.

The observed CSD of greigite from the Łąka specimen could be simulated in the same way as was done for the MMP greigite. Crystals that formed in one nucleation cycle were subjected to random growth in the open system. The rate of growth affects the evolution of the shape of the CSD. Since there is an essential randomness in the calculation, the nucleation cycle does not always produce the same initial CSD, causing some variation in the rate coefficient that can be used in the subsequent random-growth process to produce the best-fitting CSD. Therefore, even though slightly different rate coefficients were applied for the MMP and the Łąka specimen (1.05 and 1.2, respectively, for the curves shown in Fig. 8), this does not necessarily mean that the Łąka crystals grew faster than the greigite magnetosomes in the MMP.

The Fe sulfides from the Michalovce rock seem to have followed a pathway of growth that is different from the processes that formed the MMP and the Łąka greigite populations. The CSD of the Michalovce specimen could be simulated using a combination of surface-controlled and supply-controlled growth processes in an open system. The crystals reached a mean size of about 20 to 25 nm by surface-controlled growth, yielding a lognormal CSD (β^2 = 0.23); during this phase the growth was not limited by the supply of nutrients to the crystal surface. As the crystals grew and

their surface areas increased, the demand for supply increased exponentially. Eventually, at a mean size of about 25 nm the growth mechanism changed from surface- to supply- (or transport-) controlled growth, a mechanism that basically preserved the β^2 value of the previous distribution. This type of crystal growth history is common in both natural and synthetic specimens in which crystal populations having lognormal CSDs occur (Kile & Eberl, 1999).

Implications for the formation of BCM greigite and comparison with BCM magnetite

The Gaussian shape of the average CSD of the MMP greigite (Fig. 3c) is surprising, since all previous measurements on crystals from magnetotactic bacteria showed negatively skewed CSDs (Devouard *et al.*, 1998; Meldrum *et al.*, 1993a; 1993b; Pósfai & Arató, 2000); however, these asymmetric size distributions were all obtained from magnetite, not from Fe sulfides. The characteristically different shapes of magnetite and greigite CSDs can be attributed to distinct BCM processes in the two major types of magnetotactic bacteria. Whereas Ostwald ripening was found to be the most likely growth process for the negatively skewed magnetite CSDs (Eberl & Frankel, 1999), greigite magnetosomes have grown by a random process. It is interesting that the sizes of both individual cells and entire multicellular aggregates also exhibit nearly Gaussian distributions (Lins & Farina, 1999).

A magnetosome membrane surrounds the crystals in magnetite-producing species (Gorby *et al.*, 1988) and is thought to be responsible for the strict control over the size and morphology of magnetite. In the sulfide-producing species, however, the existence of a magnetosome membrane has yet to be confirmed (Bazylinski, 1999). Further studies should address the question whether the lack of a membrane may be the reason for the random growth and unconstrained shapes of Fe sulfide magnetosomes.

Possible origins of Fe sulfides from the two rock samples

Greigite grains from the Łąka marl are similar to those from the MMP in several aspects. Greigite crystals in both samples exhibit characteristic spotty contrast in the TEM; the Łąka CSD is characterized by small values of skewness (and β^2) and standard deviation, and a mean that is only about twice as large as the mean of the MMP greigite distribution (Table 1). Since the single-domain range in greigite extends to much larger sizes than in magnetite (Hoffmann, 1992), all greigite crystals in the Łąka rock are single magnetic domains. Fe sulfides having similar sizes have been observed in magnetotactic bacteria other than the MMP (for example, in Fig. 6 in Pósfai *et al.*, 1998b). The CSDs of both the MMP and the Łąka greigite could be simulated using the same crystal-growth mechanism (random growth in an open system), indicating that similar processes could have formed these two sets of crystals.

The mean size and the aggregated occurrence of Fe sulfide grains in the Michalovce sample are consistent with experimental data for framboidal pyrite (Wilkin *et al.*, 1996). "Framboids" are spherical aggregates of mostly submicrometer, euhedral crystals that represent the dominant morphological form of pyrite in marine sediments. According to calculations by Wilkin & Barnes (1997), framboids form as a result of magnetic interactions between greigite crystals that are precursors to pyrite. When greigite converts to pyrite, the framboidal morphology is preserved. However, recent results by Butler *et al.* (2000) indicate that a ferrimagnetic precursor is not necessary for the self-organization of pyrite crystals into framboids. In any case, mixed greigite/pyrite framboids have been observed in marine sediments (Bonev *et al.*, 1989; Roberts & Turner, 1993). The sizes of the Michalovce Fe sulfides, their euhedral morphologies, and the occurrence of both greigite and pyrite in the same aggregates are all consistent with our current knowledge of Fe sulfide framboids. The simulated crystal growth mechanism (surface-controlled growth followed by supply-controlled growth in an open system) is also feasible for the growth of framboidal Fe sulfides.

Although framboidal pyrite can be synthesized inorganically (Sweeney & Kaplan, 1973; Butler *et al.*, 2000), in natural sediments the chemical environment that is necessary for Fe sulfide formation is created by sulfate-reducing bacteria (Berner, 1984). Since the locus of sulfate reduction is the surface of bacteria, the Fe sulfide crystals can occur in association with bacteria, but outside their cells. Thus, framboidal Fe sulfide can be regarded as formed by BIM processes.

Based on our TEM observations and simulations of crystal growth mechanisms, bacterial greigite from the MMP and greigite from the Łąka marl specimen have similar origins, indicating that the Łąka greigite likely formed by biologically controlled mineralization. Greigite and pyrite

crystals in the Michalovce rock sample formed as a result of BIM processes. The analysis and simulation of CSDs are useful tools for studying the possible biogenic origin of Fe sulfides in geological specimens.

Acknowledgements: We thank Dennis Eberl for making the GALOPER program available, and acknowledge the constructive reviews by Marcos Farina and Bertrand Devouard. This research was supported by grants from the Hungarian Academy of Sciences (AKP #98-94 2.5) and the Hungarian Science Research Fund (OTKA T029805). PRB and RBF acknowledge support from the U.S. National Science Foundation.

References

Arató, B., Cziner, K., Pósfai, M., Márton, E., Márton, P. (2000): Magnetite and greigite from magnetotactic bacteria and from sedimentary rocks: Size distributions and microstructures. *10th Goldschmidt Conference, J. Conf. Abstr.*, **5**, 153.

Bazylinski, D.A. (1999): Synthesis of the bacterial magnetosome: The making of a magnetic personality. *Internatl. Microbiol.*, **2**, 71-80.

Bazylinski, D.A. & Moskowitz, B.M. (1997): Microbial biomineralization of magnetic iron minerals. *In* Banfield, J.F. & Nealson, K.H., (ed.): "Geomicrobiology: Interactions between microbes and minerals". Washington, D.C.: Mineralogical Society of America, **35**, 181-223.

Berner, R.A. (1984): Sedimentary pyrite formation: An update. *Geochim. Cosmochim. Acta*, **48**, 605-615.

Bonev, I.K., Khrischev, K.G., Neikov, H.N., Georgiev, V.M. (1989): Mackinawite and greigite in iron sulphide concretions from Black Sea sediments. *Compt. Rend. Acad. Bulg. Sci.*, **42**, 97-100.

Butler, I., Rickard, D., Grimes, S. (2000): Framboidal pyrite: Self organisation in the Fe-S system. *J. Conf. Abstr.*, **5**, 276-277.

DeLong, E.F., Frankel, R.B., Bazylinski, D.A. (1993): Multiple evolutionary origins of magnetotaxis in bacteria. *Science*, **259**, 803-806.

Devouard, B., Pósfai, M., Hua, X., Bazylinski, D.A., Frankel, R.B., Buseck, P.R. (1998): Magnetite from magnetotactic bacteria: Size distributions and twinning. *Am. Mineral.*, **83**, 1387-1399.

Devouard, B., Pósfai, M., Bazylinski, D.A., Frankel, R.B., Hua, X., Buseck, P.R, (2000): Crystal size distributions of magnetites from magnetotactic bacteria. *Biogenic Iron Minerals Symposium 2000, Acta Miner.-Petr. Szeged*, **41B**, 19-20.

Eberl, D.D. & Frankel, R.B. (1999): Crystal size distributions as magnetite biomarkers. *Annu. Meeting of the Geol. Soc. Am., Abstracts*, **31**, A379.

Eberl, D.D., Drits, V.A., Srodon, J. (1998): Deducing growth mechanisms for minerals from the shapes of crystal size distributions. *Amer. J. Sci.*, **298**, 499-533.

–, –, – (2000): User's guide to GALOPER - a program for simulating the shapes of crystal size distributions - and associated programs. *U. S. Geol. Survey Open File Report*, **OF 00-505**, 44 p. (ftp://brrcrftp.cr.usgs.gov /pub/ddeberl/pc_version/ GALOPER/)

Farina, M., Esquivel, D.M.S., Lins de Barros, H.G.P. (1990): Magnetic iron-sulphur crystals from a magnetotactic microorganism. *Nature*, **343**, 256-258.

Frankel, R.B., Bazylinski, D.A., Johnson, M.S., Taylor, B.L. (1997): Magneto-aerotaxis in marine coccoid bacteria. *Biophys. J.*, **73**, 994-1000.

Gorby, Y.A., Beveridge, T.J., Blakemore, R.P. (1988): Characterization of the bacterial magnetosome membrane. *J. Bacteriol.*, **170**, 834-841.

Heywood, B.R., Bazylinski, D.A., Garratt-Reed, A., Mann, S., Frankel, R.B. (1990): Controlled biosynthesis of greigite (Fe_3S_4) in magnetotactic bacteria. *Naturwiss.*, **77**, 536-538.

Heywood, B.R., Mann, S., Frankel, R.B. (1991): Structure, morphology and growth of biogenic greigite (Fe_3S_4). *Mat. Res. Soc. Symp. Proc.*, **218**, 93-108.

Hoffmann, V. (1992): Greigite (Fe_3S_4): magnetic properties and first domain observations. *Phys. Earth Planet. Int.*, **70**, 288-301.

Jelinovska, A., Tucholka, P., Guichard, F., Lefévre, I., Badaut-Trauth, D., Chalié, F., Gasse, F., Tribovillard, N., Desprairies, A. (1998): Mineral magnetic study of Late Quaternary South Caspian Sea sediments: Palaeoenvironmental implications. *Geophys. J. Int.*, **133**, 499-509.

Kile, D.E. & Eberl, D.D. (1999): Crystal growth mechanisms in miarolitic cavities in the Lake George ring complex and vicinity, Colorado. *Am. Mineral.*, **84**, 718-724.

Krs, M., Novák, F., Krsová, M., Pruner, P., Kouklíková, L., Jansa, J. (1992): Magnetic properties and metastability of greigite-smythite mineralization in brown-coal basins of the Krusné hory Piedmont, Bohemia. *Phys. Earth Planet. Int.*, **70**, 273-287.

Lins, U. & Farina, M. (1999): Organization of cells in magnetotactic multicellular aggregates. *Microbiol. Res.*, **154**, 9-13.

Lins, U., Freitas, F., Keim, C.N., Farina, M. (2000): Electron spectroscopic imaging of magnetotactic bacteria: Magnetosome morphology and diversity. *Microsc. Microanal.*, **6**, 463-470.

Lowenstam, H.A. & Weiner, S. (1989): "On biomineralization". Oxford, New York: Oxford University Press.

Mann, S., Sparks, N.H.C., Frankel, R.B., Bazylinski, D.A., Jannasch, H.W. (1990): Biomineralization of ferrimagnetic greigite (Fe_3S_4) and iron pyrite (FeS_2) in a magnetotactic bacterium. *Nature*, **343**, 258-261.

McKay, D.S., Gibson, E.K., Jr., Thomas-Keprta, K.L., Vali, H., Romanek, C.S., Clemett, S.J., Chillier,

X.D.F., Maechling, C.R., Zare, R.N. (1996): Search for past life on Mars: Possible relic biogenic activity in Martian meteorite ALH84001. *Science*, **273**, 924-930.

Meldrum, F.C., Mann, S., Heywood, B.R., Frankel, R.B., Bazylinski, D.A. (1993a): Electron microscopy study of magnetosomes in a cultured coccoid magnetotactic bacterium. *Proc. Roy. Soc. Lond.*, **B251**, 231-236.

– , – , – , – , – (1993b): Electron microscopy study of magnetosomes in two cultured vibrioid magnetotactic bacteria. *Proc. Roy. Soc. Lond.*, **B251**, 237-242.

Morse, J.W., Millero, F.J., Cornwell, J.C., Rickard, D. (1987): The chemistry of the hydrogen sulfide and iron sulfide systems in natural waters. *Earth-Sci. Rev.*, **24**, 1-42.

Pósfai, M. & Arató, B. (2000): Magnetotactic bacteria and their mineral inclusions from Hungarian freshwater sediments. *Acta Geol. Hung.*, **43**, in press.

Pósfai, M., Buseck, P.R., Bazylinski, D.A., Frankel, R.B. (1998a): Reaction sequence of iron sulfides in bacteria and their use as biomarkers. *Science*, **280**, 880-883.

– , – , – , – (1998b): Iron sulfides from magnetotactic bacteria: Structure, composition, and phase transitions. *Am. Mineral.*, **83**, 1469-1482.

Rickard, D. (1995): Kinetics of FeS precipitation. 1. Competing reaction mechanisms. *Geochim. Cosmochim. Acta*, **59**, 4367-4380.

– (1997): Kinetics of pyrite formation by the H_2S oxidation of Fe(II) monosulfide in aqueous solutions between 25 and 125 C: The rate equation. *Geochim. Cosmochim. Acta*, **61**, 115-134.

Rickard, D. & Luther, G.W., III (1997): Kinetics of pyrite formation by the H_2S oxidation of Fe(II) monosulfide in aqueous solutions between 25 and 125 C: The mechanism. *Geochim. Cosmochim. Acta*, **61**, 135-147.

Roberts, A.P. (1995): Magnetic properties of sedimentary greigite (Fe_3S_4). *Earth Planet. Sci. Lett.*, **134**, 227-236.

Roberts, A.P. & Turner, G.M. (1993): Diagenetic formation of ferrimagnetic iron sulphide minerals in rapidly deposited marine sediments, South Island, New Zealand. *Earth Planet. Sci. Lett.*, **115**, 257-273.

Sagnotti, L. & Winkler, A. (1999): Rock magnetism and palaeomagnetism of greigite-bearing mudstones in the Italian peninsula. *Earth Planet. Sci. Lett.*, **165**, 67-80.

Schoonen, M.A.A. & Barnes, H.L. (1991): Reactions forming pyrite and marcasite from solution: II. Via FeS precursors below 100°C. *Geochim. Cosmochim. Acta*, **55**, 1505-1514.

Srodon, J., Eberl, D.D., Drits, V.A. (2000): Evolution of fundamental-particle size during illitization of smectite and implications for reaction mechanism. *Clays Clay Mineral.*, **48**, 446-458.

Stanjek, H., Fassbinder, J.W.E., Vali, H., Wägele, H., Graf, W. (1994): Evidence of biogenic greigite (ferrimagnetic Fe_3S_4) in soil. *Eur. J. Soil. Sci.*, **45**, 97-103.

Sweeney, R.E. & Kaplan, I.R. (1973): Pyrite framboid formation: Laboratory synthesis and marine sediments. *Geology*, **68**, 618-634.

Thomas-Keprta, K.L., Bazylinski, D.A., Kirschvink, J.L., Clemett, S.J., McKay, D.S., Wentworth, S.J., Vali, H., Gibson, E.K., Jr., Romanek, C.S. (2000): Elongated prismatic magnetite crystals in ALH84001 carbonate globules: Potential Martian magnetofossils. *Geochim. Cosmochim. Acta*, **64**, 4049-4081.

Wilkin, R.T. & Barnes, H.L. (1997): Formation processes of framboidal pyrite. *Geochim. Cosmochim. Acta*, **61**, 323-339.

Wilkin, R.T., Barnes, H.L., Brantley, S.L. (1996): The size distribution of framboidal pyrite in modern sediments: An indicator of redox conditions. *Geochim. Cosmochim. Acta*, **60**, 3897-3912.